Sensors and Materials, Vol. 36, No. 8 (2024) 3625–3636
MYU Tokyo

S & M 3754

Thermal Performance of a Ball Bearing System Operating at High Speed with a Circulating Oil Lubrication Module

Chih-Ming Chen,[1] Huey-Ling Chang,[2*] Chun-Ying Lee,[3] and Zi-Xuan Huang[1]

[1]Department of Mechanical Engineering, National Chin-Yi University of Technology,
No. 57, Sec. 2, Zhongshan Rd., Taiping Dist., Taichung 41170, Taiwan
[2]Department of Chemical and Materials Engineering, National Chin-Yi University of Technology,
No. 57, Sec. 2, Zhongshan Rd., Taiping Dist., Taichung 41170, Taiwan
[3]Department of Mechanical Engineering, National Taipei University of Technology,
No. 1, Sec. 3, Zhongxiao E. Rd., Daan Dist., Taipei 10608, Taiwan

(Received February 1, 2024; accepted July 5, 2024)

Keywords: ball bearing, oil lubrication system, lubrication oil, viscosity, preload

Bearings are common components used in the transmission system of tool machinery and linear drive equipment. With increasing demand for higher efficiency and faster production under the required accuracy, the control of bearing temperature rise under high operational speed becomes a critical issue. The improper control of temperature rise can lead to the thermal deformation and life reduction of the machinery. Conventionally, a circulating oil lubrication system is utilized with journal bearings. In this study, a similar lubrication system was adopted for the ball bearing with a retrofit design. Three control factors, i.e., rotational speed, bearing preload, and the viscosity of the lubricant used, were chosen to study their effects on the temperature performance of the proposed lubrication system. Experimental measurements showed that the lubrication system was able to lower the temperature rise of the bearing considerably compared with its unlubricated counterpart, especially at high rotational speeds. Even with the enhanced cooling from the oil circulation system, temperature rise still increased with rotational speed. However, with increased preload, the temperature rise first dropped and then increased owing to the different contact characteristics of the balls and rings of the bearing. A fitted function for the temperature rise of the bearing under different operational conditions was demonstrated to have a prediction accuracy within 3%. Therefore, the retrofitted bearing oil cooling system should be applicable in the design of high-speed machinery for industry.

1. Introduction

Because of the increasing demand for the better surface finish and higher productivity of machine parts, machine tools and motion-controlled platforms are required to operate under high speed with steady performance. The high-speed spindle constitutes one of the critical subsystems of such machinery. Moreover, the most challenging part of the high-speed spindle lies in the bearing assembly because the temperature rise always degrades the bearing stiffness

*Corresponding author: e-mail: chl@ncut.edu.tw
https://doi.org/10.18494/SAM5017

ISSN 0914-4935 © MYU K.K.
https://myukk.org/

and produces thermal deformations.[1] Journal bearings with their fluid-lubricated nature are specifically suitable for this high-speed application. However, the performance of the journal bearings still requires careful design considerations of, for example, the oil groove size and configuration,[2] oil groove surface roughness,[3] bearing material properties,[4] spindle bending rigidity,[5] the axial displacement of the radial bearing,[6] and the rigidity change due to thermal deformation.[7] A real-time feedback control system of the bearing with a forced fluid cooling system consisting of different cooling circuits can better adapt to different working scenarios and maintain high reliability under various service conditions, although it is more expensive.[8]

Although journal bearings are more applicable in high-speed applications, their low load bearing capability and higher friction loss under low operational speed are difficult to overcome. In this regard, roller bearings with very low friction in operation are superior to their sliding counterparts. Moreover, the preload of the roller bearing can be applied to eliminate the backlash and tune the rigidity of the bearing. Therefore, the roller bearing, especially the ball bearing, is frequently adopted in various applications. However, in high-speed or high-preload operation, the frictional heat power increases considerably. To control the effects of the resulting temperature rise, such as inaccuracy due to thermal deformation[9] and instability due to preload change,[9,10] methods such as the thermal deformation compensation[9,11] and implementation of a cooling system[8,10,12] have been proposed. A simple method of cooling enhancement using grease infill may not inhibit the temperature rise because of increased damping.[13]

The aforementioned cooling system designs for roller bearings usually take into consideration the spindle system. The circuit of cooling fluid is restrained within the mounting body to loop around the spindle and the bearing. The heat of the bearing is still dissipated as the conduction heat transferred out of the outer ring from the inner ring. This limited cooling capability could inhibit the operation of the system under high rotational speed. Therefore, an oil cooling system with a lubricant flow path directly into the inner ring space was investigated in this study. This proposed cooling system, which is not seen in the literature to the best of our best knowledge, was tested experimentally with different operational parameters of bearing preload, the viscosity grade of oil, and spindle rotational speed.

2. Experimental Methods

2.1 Bearing and mounting system

Two angular ball bearings (NSK 7208A) in a duplexing arrangement with face-to-face (DF) mounting, which can accommodate heavy radial and thrust loads from either direction, were adopted in this study, as shown in Fig. 1. Four major components of the ball bearing were the inner ring, outer ring, balls, and retainer. To secure the required mounting assembly, the machined parts shown in Fig. 1 were manufactured with high precision. For example, the flatness of the contact plane, the roundness of the contact circular hole, the perpendicularity between the hole and the contact plane, were all within 5 μm while the concentricity was controlled below 10 μm. The chosen bearings had good loading capacity in both radial and axial

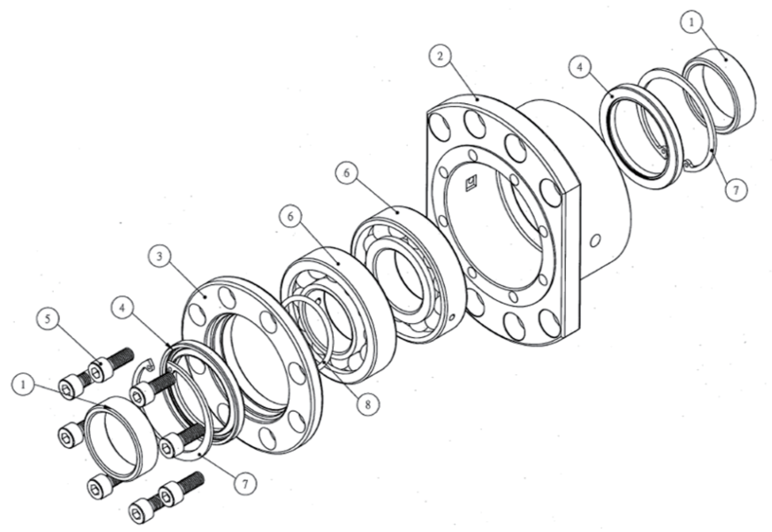

Fig. 1. Exploded drawing of the proposed bearing mount assembly. 1: spindle adapter, 2: mounting body, 3: bearing pressing cap, 4: oil seals, 5: fastening bolts, 6: angular ball bearings, 7: snap ring, and 8: spacer ring.

directions as well as superior stiffness to withstand loading deformation and maintain positioning accuracy.

As clearly seen in Fig. 1, the bearing mount consisted of several components. Because a retrofitted oil circulation system was to be used with the assembly, two oil seals were installed on both sides of the bearing duplex to prevent oil leakage from the mounting. Furthermore, in the mounting body, two holes were drilled as sites of connection to the oil circulation system. After assembly, these holes were aligned with their counterparts in the outer rings of the bearing such that the lubricating oil could flow through the housing and outer ring holes on one side, enter the space between the rings to cool the balls and race tracks, and finally pass through the holes on the other side of the housing back to the circulation system.

2.2 Lubrication oils

There are various lubrication oils available for industrial applications. Among the mechanical properties of lubrication oils, viscosity is the most relevant to their lubrication performance. Higher viscosity can provide more loading capability while lower viscosity can present less frictional loss.(14,15) The lubrication oils employed in this study comprised the same base oil (Mobil Velocite #10) and three different amounts of additives to tune their viscosities to 5.06, 11.0, and 16.5 cSt at room temperature. However, viscosity always varies with temperature as well as other factors. As an initial investigation on this lubrication and cooling system and to control the temperature rise within an acceptable range, the effect of temperature on oil viscosity was not taken into account.

2.3 Oil circulating and cooling system

Figure 2 presents the schematic diagram of the proposed oil cooling system. The oil from the condenser tank is pressurized by the hydraulic pump through the transmission tube to the inlet port of the bearing mount. Then, the aforementioned oil passage provides flow routes for the oil to carry the heat generated during bearing operation to the outlet port. The oil at elevated temperature returns to the condenser through the return transmission tube owing to the absorbed heat. Ideally, the absorbed heat carried by the oil is dissipated in the condenser and the oil temperature decreases accordingly. However, the cooling power of the oil system is designed with a compromise between performance and cost. Depending on the thermal heat generated under different operational conditions, the oil temperature may change in different experiments. Therefore, two thermocouples of type K are installed in the inlet and outlet tubes to record the oil temperatures at a sampling rate of 100 Hz with a data acquisition system. The specifications of this oil cooling system are as follows: the nominal output pressure head and volumetric flow rate are 3.0 kgf/cm^2 and 8.0 L/min, respectively, the diameter of all transmission tubes is 20.955 mm, and the volume of the condenser tank is 35 L.

2.4 Performance tester of high-speed spindle

Figure 3 shows the schematic diagram of the high-speed spindle performance tester used in this study. The spindle, assembled with the bearing block as shown in Fig. 1, and the oil cooling system were installed on the test rig. It should be mentioned that in order to obtain the required preload in the bearings, the thickness of the spacer ring was carefully selected. Different preloads were obtained by using spacer rings with different thicknesses. Moreover, a precision locknut assembled on top of the mounting assembly was tightened to the required torque to maintain the set preload. The temperature of this locknut is examined in the results reported later. In addition to the two thermocouples installed in the oil transmission tubes for temperature measurements under different operational conditions, temperatures at other locations, such as the spindle, locknut, and inner ring of the bearing, were measured using an infrared camera. During the rotational experiments, the spindle was driven by an induction servomotor of 1.5 kW, which had a maximum rotational speed of 24000 rpm.

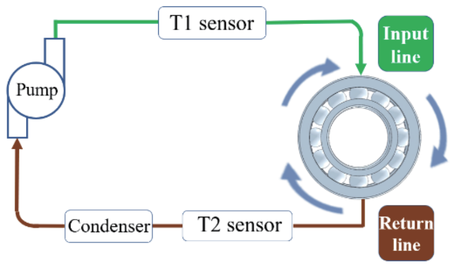

Fig. 2. (Color online) Schematic diagram of the proposed oil cooling system.

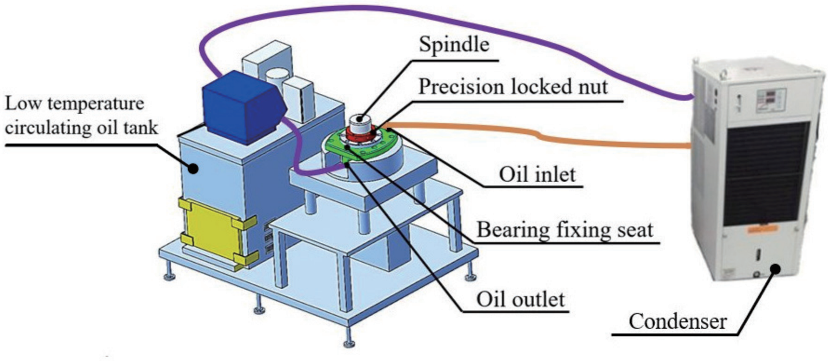

Fig. 3. (Color online) Schematic diagram of the high-speed spindle performance tester used in this study.

3. Results and Discussion

In this study, we focus on the temperature effect in terms of the operational parameters of the bearing, i.e., preload, oil viscosity index, and spindle rotational speed. Table 1 presents the operational parameters of the experiments conducted herein. The ball bearing used in this study had a basic dynamic load rating of 35.5 kN such that the preload in the range of 7–12 kN was used. Although the ball bearing is usually not intended to serve under the combination of high load and high speed, the high rotational speed from 8000 to 12000 rpm was selected to test an extreme operational situation.

3.1 Conventional ball bearing mounting without oil cooling system

An experiment using the bearing mounting without the circulating oil cooling system was performed first as the control experiment. Since a poor performance was expected, the least challenging operation parameters among those listed in Table 1 were adopted, i.e., a place of 7000 N, an oil viscosity of 16.5 cSt, and different rotational speeds. To prevent damage to the test equipment, the experiment was aborted when the measured temperature exceeded 75 ℃. Figure 4 shows the measured temperature histories of the bearing inner ring at three different spindle speeds. It is seen that the temperature increased rapidly at the beginning of the testing period at all three speeds. After 20 min, the trend of the temperature rise remained the same but with a much lower slope. It seemed that the increased heat dissipation from the hotter mounting surface was able to reduce the rate of temperature rise from frictional heat. However, because of the higher heat generation rate at higher rotational speed, the heat dissipation from the mounting surface was not able to keep up. Therefore, the measured temperature exceeded 80 ℃ in 40 min and the test was aborted as planned. The results demonstrated that the conventional ball bearing was not suitable for service at speeds higher than 10000 rpm even within a short period.

Table 1
Operational parameters of the experiments conducted in this study.

Operational parameter	Level 1	Level 2	Level 3
Spindle rotational speed (rpm)	8000	10000	12000
Oil viscosity (cSt)	5.06	11.0	16.5
Bearing preload (N)	7000	10000	13000

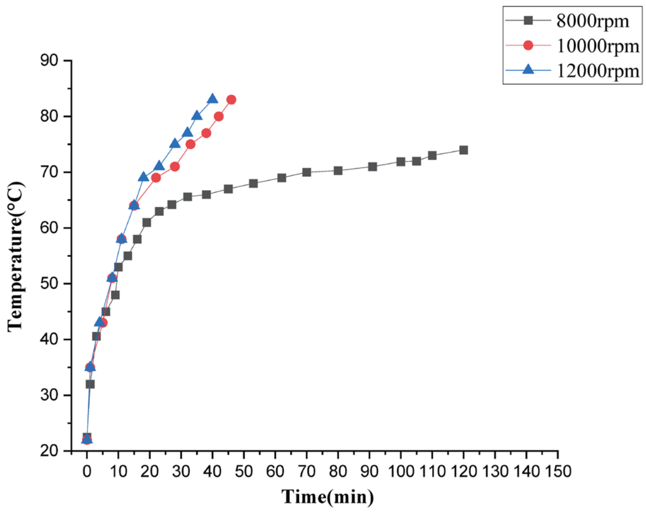

Fig. 4. (Color online) Temperature history of the bearing inner ring for the conventional bearing mounting without oil cooling system. The bearings were operating at a preload of 7000 N, an oil viscosity of 16.5 cSt, and different spindle speeds.

3.2 Effect of oil viscosity

The effect of using oils with three different viscosities was investigated under a preload of 7000 N and a rotational speed of 8000 rpm for the proposed oil-cooled bearing mounting. Figure 5 presents the temperature history at the outlet of oil circulation from the mounting block. It is clearly seen that for all three oil viscosities, the oil temperature rapidly reached the steady state within 20 min. Therefore, the steady-state temperatures at different locations of the bearing mount were measured and are shown in Table 2. Note that all the reported data are the average of three repeated measurements with a coefficient of variance less than 5%.

Table 2 shows the temperatures obtained before and after the experiment, and the corresponding temperature rises at different locations of the bearing mount. The results clearly reveal that after the experiment, the temperature rises at all locations increase with the viscosity of the oil used. Although the more viscous oil can provide better load bearing capability, the higher viscosity also results in higher frictional drag and, consequently, higher generated heat. Moreover, the higher drag causes a larger pressure drop in the oil circulation circuit. Therefore, the reduced volumetric flow rate decreases the speed, which leads to an increase in the amount of heat generated. All these effects contribute to the higher temperature rise when using oil with higher viscosity. Among different locations, the temperature rise at the bearing inner ring was

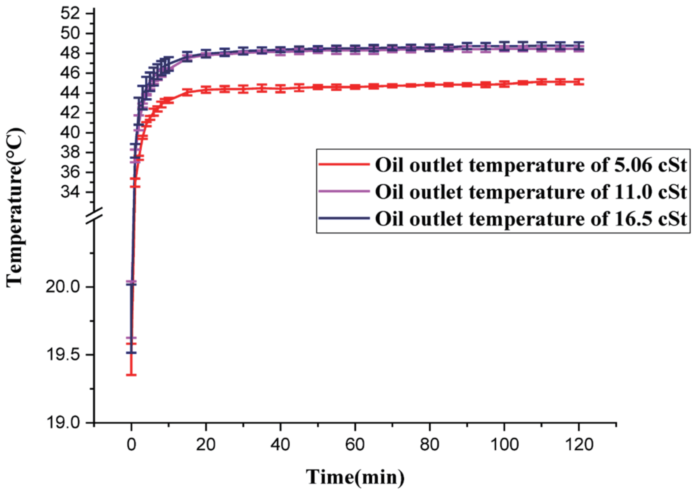

Fig. 5. (Color online) Temperature history at the outlet of the proposed bearing mounting with oil cooling system. The bearings were operating at a preload of 7000 N, a speed of 8000 rpm, and different oil viscosities.

Table 2
The steady state temperatures of the bearing mounting operated at a preload of 7000 N, speed of 8000 rpm, and different oil viscosities.

Location	Condition	Viscosity (cSt)		
		5.06	11.0	16.5
Spindle	Before	22.70	22.77	22.50
	After	31.93	32.83	34.62
	Temp. rise	9.23	10.06	12.12
Locknut	Before	22.29	22.20	22.76
	After	39.79	42.74	44.69
	Temp. rise	17.50	20.54	21.93
Bearing inner ring	Before	21.93	22.42	22.70
	After	49.37	52.46	54.18
	Temp. rise	27.44	30.04	31.48
Oil	Before (inlet)	19.50	19.53	19.67
	After (outlet)	45.10	48.47	48.77
	Temp. rise	25.60	28.94	29.10

more prominent than these at other positions. It is understood that the inner ring is closest to the source of frictional heat and most distant from the bearing mount surface. Therefore, it is most vulnerable to overheating damage in the bearing system.

3.3 Effect of spindle speed

To simulate the worse situation, the maximum preload of 13000 N was chosen from the operational parameters in Table 1. In accordance with the heavier loading, more viscous oil is usually employed to match the load bearing capability in engineering practice. Therefore, oil with the viscosity of 16.5 cSt. was selected in this experiment. Figure 6 shows the measured time history for this bearing operating with different spindle speeds. As in the previous results shown in Fig. 5, the temperature at the oil outlet of the bearing block rapidly rose from the initial value

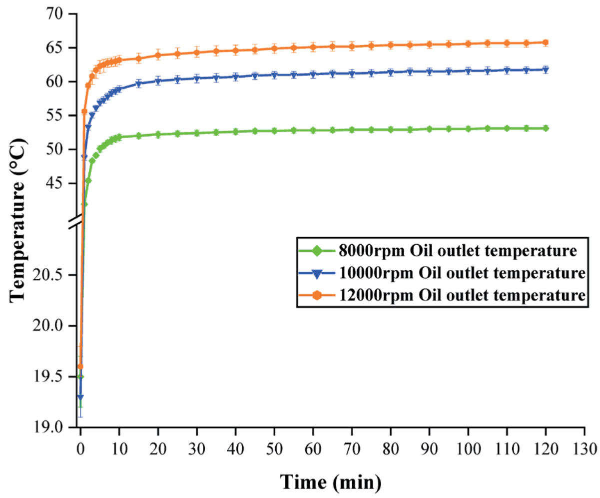

Fig. 6. (Color online) Temperature history at the outlet of the proposed bearing mounting with oil cooling system. The bearings were operating at a preload of 13000 N, an oil viscosity of 16.5 cSt, and different spindle speeds.

to a nearly stable value in 20 min. Moreover, the stable temperature increased with the rise in spindle speed, as expected from the higher frictional power at higher speed. Along with the stable temperature rise at the oil outlet site, those at other locations are listed in Table 3.

As seen from the results in Table 3, at all locations, temperature rises increase with the rotational speed. The temperatures are within the normal temperature range of the lubrication oil, which demonstrates the satisfactory performance of the proposed system. Note that although the inner ring usually had the highest working temperature, at the high preload of 13000 N, the position of the highest temperature changed from the inner ring to the oil outlet port at spindle speeds of 10000 and 12000 rpm. This may be due to the greater convection cooling from the inner ring surface at high rotational speeds while the surface was at a higher temperature. As mentioned previously, the temperatures at the inner ring were measured on the surface IR image, while the outlet temperature was measured directly from the oil flowing out of the bearing mount body. Therefore, the oil temperature at the outlet port should be a more realistic indication of the bearing temperature in a heavy working environment.

3.4 Effect of bearing preload

Three different preloads were selected while the other operational parameters were fixed at a spindle speed of 12000 rpm and an oil viscosity of 16.5 cSt for this experiment. Table 4 shows the measured stable temperatures at different locations of the bearing mount system. Note that the temperature rise did not change monotonically with the preload rise from 7000 to 13000 N. Instead, the temperature rise decreased slightly from 7000 to 10000 N and rose again at 13000 N. At the low preload of 7000 N, more clearance between parts in contact might exist, and more sliding may have occurred within the rolling motion. As the preload first increased, the contact between running counterparts improved and the sliding motion diminished. Thus, the amount of frictional heat generated decreased. When the preload was further increased, the contact area

Table 3
Steady-state temperatures of the bearing mounting operated at preload of 13000 N, oil viscosity of 16.5 cSt, and different spindle speeds.

Location	Condition	Spindle speed (rpm)		
		8000	10000	12000
Spindle	Before	23.19	23.00	23.27
	After	35.91	36.80	37.44
	Temp. rise	12.72	13.80	14.17
Locknut	Before	22.40	23.50	23.88
	After	44.39	47.30	49.42
	Temp. rise	21.99	23.80	25.54
Bearing inner ring	Before	23.21	23.36	22.64
	After	54.72	57.56	60.23
	Temp. rise	31.51	34.20	37.59
Oil	Before (inlet)	19.57	19.53	19.56
	After (outlet)	53.13	61.77	65.77
	Temp. rise	33.56	42.24	46.21

Table 4
Steady-state temperatures of the bearing mounting operated at spindle speed of 12000 rpm, oil viscosity of 16.5 cSt, and different bearing preloads.

Location	Condition	Bearing preload (N)		
		7000	10000	13000
Spindle	Before	21.92	23.52	23.27
	After	34.51	36.89	37.44
	Temp. rise	12.59	13.37	14.17
Locknut	Before	22.07	23.22	23.88
	After	47.51	47.56	49.42
	Temp. rise	25.44	24.34	25.54
Bearing inner ring	Before	22.01	23.56	22.64
	After	58.40	59.47	60.23
	Temp. rise	36.39	35.91	37.59
Oil	Before (inlet)	19.47	19.50	19.56
	After (outlet)	62.93	63.43	65.77
	Temp. rise	43.46	43.93	46.21

between the balls and the race tracks also increased. When the contact was not of a pointwise nature, sliding might occur in bearing rotation. Moreover, the hysteresis in repeated contact deformation would also contribute to heat generation. Therefore, the temperature rise increased again with larger magnitude.

3.5 Temperature predictions at inner ring and spindle

For the machinery operated at high speed, good control of the temperature rise at its main bearings is critical in ensuring its accuracy and service life. The inner ring usually has the highest temperature, which must be brought into a tolerable range in terms of safety. Moreover,

Table 5
Confirmation tests on the predictions from the curve-fitted functions of temperatures at inner ring and spindle.

Parameters			Inner ring's temperature, T_i			Spindle's temperature, T_s		
X(cSt.)	Y(rpm)	Z(N)	Measur. (°C)	Predic.(°C)	Error (%)	Measur. (°C)	Predic.(°C)	Error (%)
5.06	12000	13000	56.44	56.99	0.97	36.43	35.51	2.52
16.5	10000	13000	57.56	56.89	0.55	36.80	36.75	0.14
16.5	12000	7000	58.40	59.39	1.75	34.51	35.19	1.97

the spindle's temperature is closely related to the thermal deformation of the machinery, which is a major determinant of its accuracy. With the data measured and presented in Tables 2–4, the polynomial functions for temperature predictions were fitted using linear regressions for the temperatures at the inner ring and spindle. These predictions will be helpful to design engineers in related fields. The obtained polynomial functions with the correlation coefficient R^2 values of 0.9259 and 0.8678 are as follows.

$$T_i = 1.49\times10^{-7}X^2 + \left(2.05\times10^{-3}\right)Y^2 + \left(8.57\times10^{-8}\right)Z^2 + \left(-6.84\times10^{-4}\right)X + \left(9.88\times10^{-1}\right)Y \\ + \left(-1.98\times10^{-3}\right)Z + \left(-7.25\times10^{-5}\right)XY + 2.07\times10^{-8}XZ + 9.07\times10^{-6}YZ + 50.55 \tag{1}$$

$$T_S = -8.17\times10^{-8}X^2 + \left(-1.61\times10^{-3}\right)Y^2 + \left(-3.41\times10^{-8}\right)Z^2 + \left(2.48\times10^{-3}\right)X + 4.83\times10^{-1}Y \\ + \left(5.01\times10^{-4}\right)Z + \left(-4.56\times10^{-5}\right)XY + 1.61\times10^{-8}XZ + 1.78\times10^{-5}YZ + 13.48 \tag{2}$$

In the above equations, T_i and T_S denote the temperatures at the inner ring and spindle, whereas X, Y, and Z are the viscosity of the oil, the rotational speed of the spindle, and bearing preload, respectively. Several confirmation tests were conducted on the predictions using Eqs. (1) and (2), and the results are presented in Table 5. It is seen that for both temperatures, all the predictions are within the measurement accuracy of 3%. The curve-fitted functions of Eqs. (1) and (2) can be employed with reasonable accuracy in the performance design of this bearing mounting.

4. Conclusions

An oil circulation module for the lubrication and cooling of a ball bearing assembly in a simulated spindle system was proposed in this study. The temperature rises under different preloads and spindle rotation speeds using oils with different viscosity indices were measured in experiments to test the lubrication and cooling performance chracteristics of the proposed new design. The findings based on the measured results are summarized below.

1. Compared with the conventional lubrication practice for ball bearings, the proposed cooling and lubrication module can effectively stabilize the temperature rise to an acceptable range within 20 min, whereas its conventional counterpart revealed overheating.
2. Increasing the rotational speed always increases the temperature of the bearing system. The temperature rise not only increases the thermal deformation but also lowers the viscosity of

the oil. The former degrades the accuracy of the spindle, while the latter lowers the oil viscosity and, consequently, the load capability of the bearing. Without proper thermal management, the bearing eventually becomes overheated.

3. The temperature rise does not monotonically increase with the bearing preload. With low preload, the bearing may not have sufficient contact load to prevent the sliding contact between the ball and the race track, and the sliding friction will contribute to the frictional heat generation. The appropriate increase in preload may diminish sliding and ensure rolling contact, which would reduce heat generation. However, further increase in preload increases the contact area between the ball and the race track, inevitably causing cyclic material deformation and partial sliding in the contact region. The hysteresis of deformation and sliding friction drive the temperature to a higher level.
4. Both predicted temperature rise equations of the inner ring and spindle correlated very well with the measured data in confirmation tests. Between these two prediction equations, the spindle equation is inferior to the inner ring equation because there are more environmental disturbances between the heat generation source and the location of the spindle.

Acknowledgments

The authors are thankful for the financial support of this study through the research project from the National Science and Technology Council, Taiwan.

References

1 A. Zahedi and M. R. Movahhedy: Sci. Iran. **19** (2012) 282. https://doi.org/10.1016/J.SCIENT.2012.01.004
2 M. A. Ahmad, S. Kasolang, and R. S. Dwyer-Joyce: Tribol. Int. **74** (2014) 79. https://doi.org/10.1016/J.TRIBOINT.2014.02.012
3 J. Weber, L. Shabi, and J. Weber: Procedia CIRP **67** (2018) 81. https://doi.org/10.1016/J.PROCIR.2017.12.180.
4 J. Gong, Y. Jin, Z. Liu, H. Jiang, and M. Xiao: Tribol. Int. **129** (2019) 390. https://doi.org/10.1016/J.TRIBOINT.2018.08.035
5 D. Fedorynenko, R. Kirigaya, and Y. Nakao: Precis. Eng. **63** (2020) 187. https://doi.org/10.1016/J.PRECISIONENG.2020.02.003
6 B. Li, J. Sun, S. Zhu, Y. Fu, X. Zhao, H. Wang, Q. Teng, Y. Ren, Y. Li, and G. Zhu: Tribol. Int. **135** (2019) 397. https://doi.org/10.1016/J.TRIBOINT.2019.03.031
7 D. Chen, M. Bonis, F. Zhang, and S. Dong: Precis. Eng. **35** (2011) 512. https://doi.org/10.1016/J.PRECISIONENG.2011.02.005
8 Y. Zhang, T. Liu, W. Gao, Y. Tian, X. Qi, P. Wang, and D. Zhang: Appl. Therm. Eng. **134** (2018) 460. https://doi.org/10.1016/J.APPLTHERMALENG.2018.02.016
9 E. Creighton, A. Honegger, A. Tulsian, and D. Mukhopadhyay: Int. J. Mach. Tools Manuf. **50** (2010) 386. https://doi.org/10.1016/J.IJMACHTOOLS.2009.11.002
10 S. N. Grama, A. Mathur, and A. N. Badhe: Int. J. Mach. Tools Manuf. **132** (2018) 3. https://doi.org/10.1016/J.IJMACHTOOLS.2018.04.004
11 C. Rabréau, J. Kekula, M. Ritou, M. Sulitka, J. Shim, S. Le Loch, and B. Furet: Procedia CIRP **77** (2018) 622. https://doi.org/10.1016/J.PROCIR.2018.08.192
12 T. Lu, R. Kudaravalli, and G. Georgiou: Procedia Manuf. **21** (2018) 266. https://doi.org/10.1016/J.PROMFG.2018.02.120
13 S. Ai, W. Wang, Y. Wang, and Z. Zhao: Tribol. Int. **87** (2015) 11. https://doi.org/10.1016/J.TRIBOINT.2015.02.011
14 P. Panwar, E. Schweissinger, S. Maier, S. Hilf, S. Sirak, and A. Martini: J. Mol. Liq. **359** (2022) 119215. https://doi.org/10.1016/J.MOLLIQ.2022.119215
15 C.-Y. Huang, T. G. Murthy, and S. Chandrasekar: Procedia Eng. **79** (2014) 9. https://doi.org/10.1016/J.PROENG.2014.06.303

About the Authors

Chih-Ming Chen is a distinguished professor of the Department of Mechanical Engineering at National Chin-Yi University of Technology. His publications in the past eight years include more than 20 international journal papers, 10 journal papers, and more than 56 conference papers. Since 2008, he has obtained a total of 66 patents and implemented more than 30 industry–university programs and government-related small and medium plans. Technology transfer assists in the upgrading of industrial technology and enhances the international competitiveness of the industry, and Dr. Chen has completed more than 18 technology transfers. His industry–university cooperation project won three Outstanding Awards and one Merit Award from Taiwan's Ministry of Science and Technology. From 2010 to 2013, he participated in the largest event of the cross-strait industry, the "cross-strait workers' innovation achievements exhibition", and won the highest honor award, the "gold medal", for a total of 16 pieces of Cross-Strait Employees Innovation Achievement Exhibition "Gold Medal". (cmchentc@gmail.com)

Huey-Ling Chang received her B.S. degree from the Department of Chemical Engineering, National Cheng Kung University, Taiwan, M.S. degree from National Tsing Hua University, and Ph.D. degree from National Chiao Tung University. She is currently a professor at National Chin-Yi University of Technology. She has 53 approved patents and 49 SCI/EI international journal papers. Her research interests are in electronic packaging materials, nanocomposites, photoelectric materials, and life cycle assessment. (hlchangtc@gmail.com)

Chun-Ying Lee received his B.S. degree from the Department of Mechanical Engineering, National Taipei Institute of Technology, Taipei, Taiwan, in 1980, M.S. degree in mechanical engineering from National Sun Yat-sen University, Kaohsiung, Taiwan, in 1985, and Ph.D. degree in engineering mechanics from Michigan State University, East Lansing, MI, USA, in 1991. He is currently a professor of the Graduate Institute of Manufacturing Technology, National Taipei University of Technology, Taipei. His current research interests include smart materials, vibration control, and the supercritical carbon-dioxide-assisted electroplating process. (leech@ntut.edu.tw)

Zi-Xuan Huang received his M.S. degree from National Chin-Yi University of Technology, Taiwan, in 2023. Since 2023, he has been a research assistant at National Chin-Yi University of Technology, Taiwan. His research interests are in materials and mechanical engineering. (nikemom013@gmail.com)